



Diamond deposition on siliconized stainless steel

F. Álvarez^{a,b}, M. Reinoso^{a,c,d,*}, H. Huck^{a,c}, M. Rosenbusch^e

^a Departamento de Física, Comisión Nacional de Energía Atómica, Avda. General Paz 1499, (B1650) Gral. San Martín, Pcia. Buenos Aires, Argentina

^b Instituto Sabato, Universidad Nacional de San Martín, Comisión Nacional de Energía Atómica, Avda. General Paz 1499, (B1650) Gral. San Martín, Pcia. Buenos Aires, Argentina

^c Escuela de Ciencia y Tecnología, Universidad Nacional de San Martín, Calle 78 N° 3901, (B1653) Villa Ballester, Pcia. Buenos Aires, Argentina

^d Consejo Nacional de Investigaciones Científicas y Técnicas, Rivadavia 1917, (1033) Buenos Aires, Argentina

^e Departamento Química de Reactores, GIDAT-GAEN-Comisión Nacional de Energía Atómica, Avda. General Paz 1499, (B1650) Gral. San Martín, Pcia. Buenos Aires, Argentina

ARTICLE INFO

Article history:

Received 30 December 2009

Received in revised form 15 January 2010

Accepted 15 January 2010

Available online 25 January 2010

Keywords:

Diamond

HFCVD

Siliconization

Stainless steel

ABSTRACT

Silicon diffusion layers in AISI 304 and AISI 316 type stainless steels were investigated as an alternative to surface barrier coatings for diamond film growth. Uniform 2 μm thick silicon rich interlayers were obtained by coating the surface of the steels with silicon and performing diffusion treatments at 800 °C. Adherent diamond films with low sp² carbon content were deposited on the diffused silicon layers by a modified hot filament assisted chemical vapor deposition (HFCVD) method. Characterization of as-siliconized layers and diamond coatings was performed by energy dispersive X-ray analysis, scanning electron microscopy, X-ray diffraction and Raman spectroscopy.

© 2010 Elsevier B.V. All rights reserved.

1. Introduction

The growth of well adherent quality diamond films on steel substrates has been a main subject of research in the field of CVD diamond deposition for the last two decades. The reduced friction and wear properties of diamond as well as the improved corrosion resistance could enhance the performance and broaden considerably the scope of applications of steel tools and devices.

Direct diamond deposition on steel poses many problems difficult to overcome. The expansion mismatch between diamond films and steel substrates and the high solubility of carbon in the austenitic phase make diamond deposition at the high temperatures employed for methane–hydrogen gas mixtures unachievable [1].

In addition, direct deposition of diamond on steel leads to graphitization of the surface. This fact was originally explained by two possible mechanisms: the stabilization of sp² bonding due to the catalytic activity of the 3d shell of iron, which promotes deposition of sp² bonded carbon phases [2], and the high vapor pressure of iron which leads to contamination of the growing diamond [3,4]. Jentsch et al. [5] later reported that graphite formation during diamond deposition is directly related to a low activity of carbon ($a_c < 1$) in the gas phase and does not show correlation with either a high vapor pressure of the substrate or an unpaired electron structure. An excess of carbon diffuses into the metal phase and this leads to the

formation of cementite (Fe₃C) at the surface which acts as a diffusion barrier for carbon and promotes precipitation of graphite on the surface. As cementite decomposes, metal atoms diffuse through the graphite layer and reach the surface where they catalyze the formation of graphite [4,5].

The use of barrier coatings has proven efficient to avoid such difficulties and metal and composite coatings have been extensively studied as interlayers for diamond deposition on steels [6–15]. In some cases diffusion layers have also been shown to be a good alternative, with the added benefit of favoring good adhesion between the steel and the interlayer. Chromium, boron and carbon diffusion layers on steel have been successfully employed to enable growth of quality diamond films [16–18].

Siliconization of stainless steels has been previously studied as a way to improve hot corrosion resistance, and 50 μm thick diffused layers were found to be free of voids and adherent, despite large local stress near the coating–substrate interface [19–21]. In the present work, silicon diffusion surface layers were formed in AISI 304 and AISI 316 stainless steels in order to study their feasibility as interlayers for diamond film growth. Continuous and adherent diamond films were deposited on the diffused silicon layers by a modified hot filament assisted chemical vapor deposition (HFCVD) technique.

2. Experimental

Diamond films were deposited by a modified hot filament CVD method on different substrates.

* Corresponding author at: CNEA, Physics, Avda. General Paz 1499, (B1650) Buenos Aires, Argentina.

E-mail address: reinoso@cnea.gov.ar (M. Reinoso).

2.1. Substrates treatment

Two different types of stainless steel were used as substrates: AISI 304 SS (0.08 wt.% C, 18.8 wt.% Cr, 8 wt.% Ni, 1.4 wt.% Si, 2.3 wt.% Mn and balance Fe), and AISI 316 SS (0.08 wt.% C, 17.2 wt.% Cr, 11.7 wt.% Ni, 2.2 wt.% Mo, 1.0 wt.% Si, 2.3 wt.% Mn and balance Fe). Both substrates were polished to a final surface roughness Ra of 0.04–0.05 μm .

An amorphous-silicon (a-Si) layer was deposited by ion beam deposition (IBD). Silane (SiH_4) was employed as a source of silicon ions and the deposition energy was 2 keV. The deposited layer was about 0.1 μm thick and it was characterized by Raman spectroscopy. Then the steel was heated up in a vacuum chamber ($<10^{-6}$ mbar) for 1 h, under the same thermal conditions used for diamond deposition (800 $^\circ\text{C}$) with the aim of creating a diffusion layer. The aforesaid process was repeated until a very thin surface layer of silicon was still found after the thermal treatment.

In all cases, prior to diamond deposition, every substrate was scratched with diamond paste (0.25 μm) in order to promote nucleation; then it was ultrasonically cleaned with acetone and rinsed in isopropanol several times, in order to remove the diamond paste.

2.2. Diamond deposition

A schematic diagram of the deposition system is shown in Fig. 1. A tungsten filament of 0.8 mm diameter and 70 mm long, was heated at 2200 $^\circ\text{C}$. The substrate was located on an electrically isolated heater (800 $^\circ\text{C}$) at a distance of 10 mm from a tungsten filament. A mixture of CH_4 and H_2 was used as precursor. Two gas inlets were provided in the deposition chamber, as can be seen in Fig. 1: one close to the hot filament and the other close to the deposition region. Hydrogen was injected behind the filament while a mixture of 2% CH_4 –98% H_2 was injected close to the substrate. This configuration was shown to reduce the decomposition of CH_4 near the filament and so, to obtain diamond deposition with lower amorphous carbon contamination [22]. Both gas flows were 100 sccm and the chamber pressure was stabilized between 12 and 15 mbar.

Diamond films were also deposited on a (1 0 0) silicon wafer under the same conditions in order to compare film structure and sp^3/sp^2 carbon ratio.

2.3. Characterization

The steel samples employed as substrates were analyzed by energy dispersive X-ray spectroscopy (EDX), X-ray diffraction

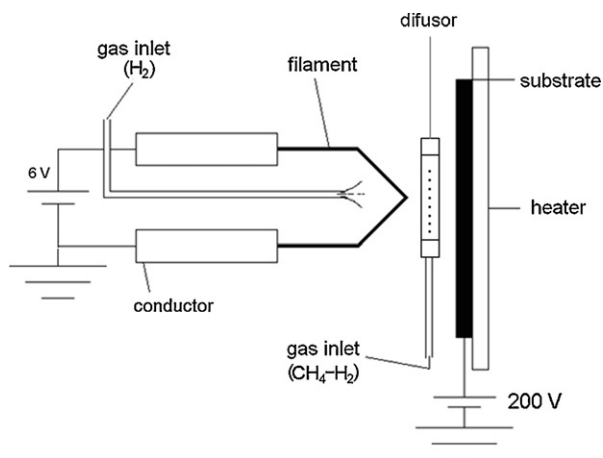


Fig. 1. Schematic diagram of the deposition system.

(XRD), and Raman spectroscopy. The deposited material was characterized by scanning electron microscopy (SEM) and Raman spectroscopy. Surface roughness parameter (R_a) was measured by a commercial surface rugosimeter/profilometer (Form Talysurf Intra 2).

Grazing-incidence X-ray diffraction was employed in order to study the crystalline structure of the films (incidence angle: 3°). The XRD patterns were recorded over the 2θ range of 10 – 90° , using $\text{Cu K}\alpha$ radiation (1.54184 \AA) at room temperature (scanning step 0.02° , 1s). Depolarized Raman spectra were taken using a commercial spectrometer with a Ar^+ laser source operating at the excitation wavelength of 514 nm. A $100\times$ objective was employed to focus the laser to a 5 μm diameter spot. The power was adjusted to minimize the temperature raised at the spot (about 20 mW). The dispersed beam was analyzed in a 180° geometry. The spectral resolution was 2.5 cm^{-1} .

3. Results and discussion

3.1. Pretreatment of stainless steel

Thin amorphous-silicon (a-Si) films were deposited on stainless steel samples and characterized by Raman spectroscopy. The Raman spectrum of an AISI 316 SS sample presents a very strong band centered at 480 cm^{-1} characteristic of Si–Si TO mode and a weak shoulder at 380 cm^{-1} (LO mode) together with an insinuation of 150 and 320 cm^{-1} bands, corresponding to TA and LA modes [23–25], as can be seen in Fig. 2(a); this spectrum confirms the presence of a-Si.

It was observed that silicon films thicker than 0.1 μm present low adherence to the substrate. Subsequent diffusion processes starting from thin silicon films of less than 0.1 μm thickness had to be carried out in order to achieve maximum silicon concentration near the surface of the stainless steel.

After the first diffusion treatment at 800 $^\circ\text{C}$ the surface of the same sample was analyzed by Raman spectroscopy and there was no indication of the presence of silicon anymore. All silicon was consumed by complete in-diffusion into the steel substrates. Silicon deposition and annealing were therefore repeated a few times (mostly twice) until Raman spectra after annealing revealed there was a silicon layer on the surface of the steel, indicating that silicon saturation was reached in the austenitic phase close to the surface. The corresponding spectrum is presented in Fig. 2(b): a band

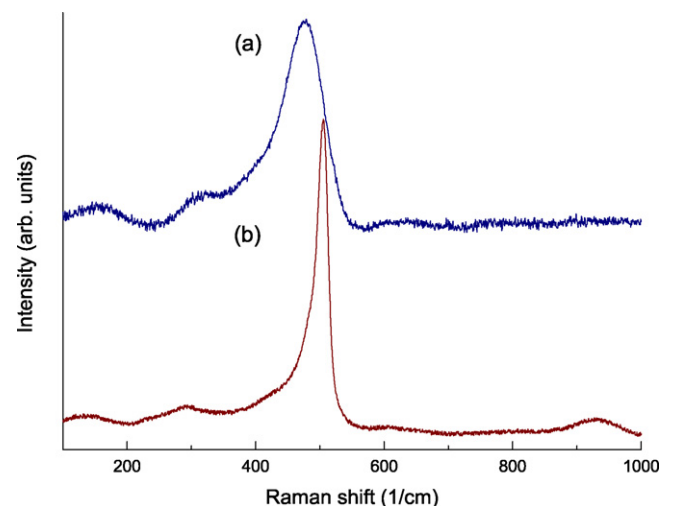


Fig. 2. Raman spectra of AISI 316 stainless steel during siliconization pretreatment: (a) after a-Si deposition, before thermal treatment and (b) after three a-Si depositions and thermal treatments.

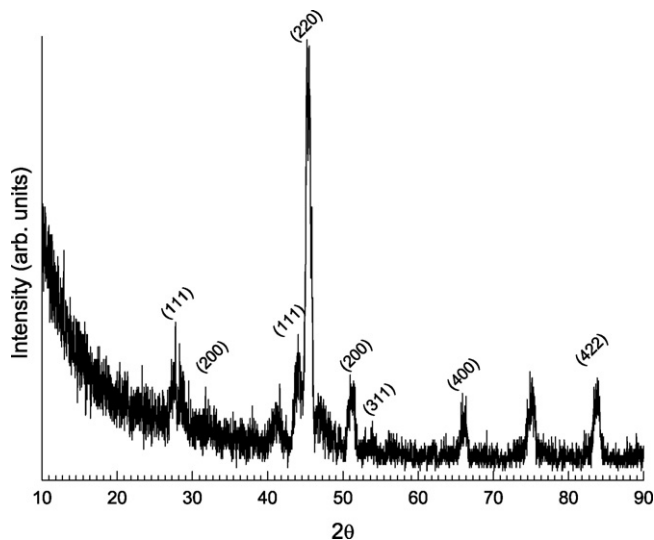


Fig. 3. X-ray diffraction pattern of a siliconized AISI 316 stainless steel.

centered at 510 cm^{-1} indicates the presence of nanocrystalline silicon (nc-Si), together with a small contribution of a-Si [23,26].

Raman spectroscopy on the surface of the samples after the diffusion annealing was used to assess that silicon was at its maximum concentration (about 5 wt.%) in the vicinity of the surface of the stainless steel samples. This assumption was later confirmed by measuring the silicon concentration near the surface of the samples by SEM-EDX.

The Raman spectra at the different stages of the substrate treatments presented the same characteristics for both AISI 316 and AISI 304 SS samples.

XRD spectra of the diffused silicon layers in AISI 316 stainless steel revealed a DO_3 microstructure corresponding to Fe_3Si , as indexed in Fig. 3; a similar spectrum was obtained for AISI 304 stainless steel, in accordance with results previously reported by Huang et al. for siliconization of AISI 304 SS [19].

Silicon concentration of the coating at different depths from the surface was obtained by SEM-EDX and is shown in Table 1. An expected concentration of silicon of 5 wt.% was measured near the surface, while a decrease to AISI 316 SS compositional values was observed at depths higher than $4\text{ }\mu\text{m}$. All measured samples presented a case depth of about $2\text{ }\mu\text{m}$. AISI 304 stainless steel samples presented similar profiles with higher silicon concentrations far from the surface which matched the Si concentration pointed out above for this steel.

A concentration of silicon of 21.7% was measured by SEM-EDX on the surface of the sample, corresponding to the contribution of the thin surface layer of silicon ($<0.05\text{ }\mu\text{m}$, as measured by a step profilometer) remaining on the surface after the diffusion process. This thin layer was not removed prior to diamond deposition and the roughness factor R_a was $0.03\text{--}0.04\text{ }\mu\text{m}$.

All three substrates, AISI 304, AISI 316 and silicon wafer, were equally scratched with diamond past ($0.25\text{ }\mu\text{m}$) and cleaned. No

Table 1

Silicon concentration obtained by SEM-EDX, at different depths from the surface of the layer.

Depth (μm)	Si concentration (wt.%)
0	21.7
0.6	5.0
2.9	1.8
8	1.1
10.3	0.96

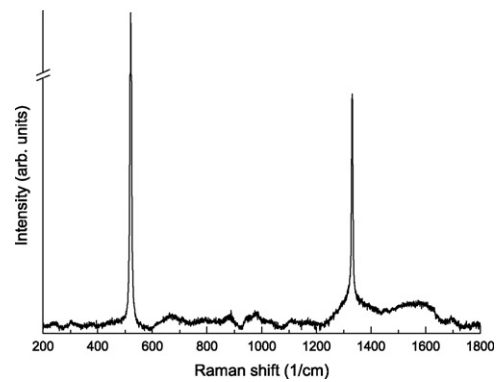


Fig. 4. Raman spectrum of a diamond film deposited on a silicon wafer.

peeling or detachment was observed on the siliconized stainless steel substrates. The roughness factor R_a after this process was about $0.03\text{--}0.04\text{ }\mu\text{m}$.

3.2. Diamond deposition and characterization

Diamond crystals were deposited on a surface of about 1 cm^2 on the different substrates. Deposition on silicon wafers resulted in continuous diamond films of about $3\text{ }\mu\text{m}$ thick and the deposition time was 3 h for all the samples. The Raman spectrum of the sample showed the characteristic peak at 1332 cm^{-1} corresponding to diamond as can be seen in Fig. 4. The intensity of the silicon peak at 520 cm^{-1} from the substrate points out the transparency of

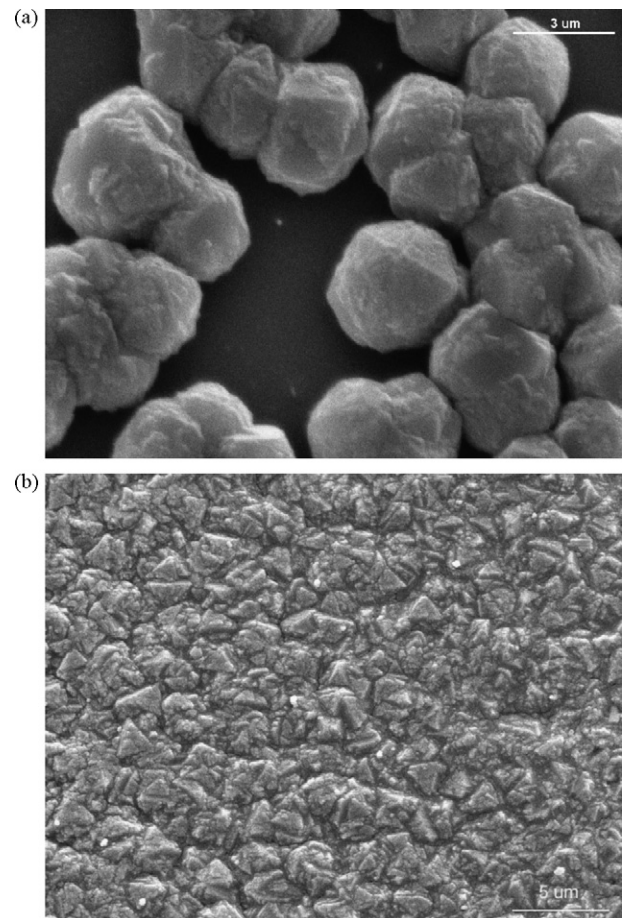


Fig. 5. SEM micrograph of: (a) isolated diamond crystals and (b) continuous diamond film deposited on a silicon wafer.

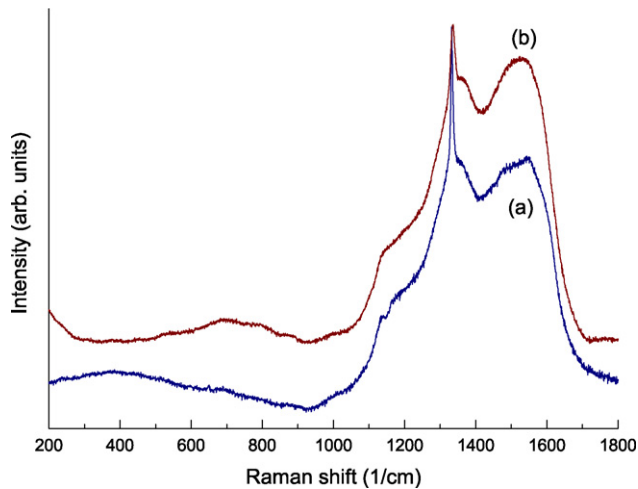


Fig. 6. Raman spectra of diamond film deposited on AISI 316 (a) and AISI 304 (b) stainless steel.

the diamond film. This fact together with the small signal of amorphous carbon reveals the good quality of the deposited film. Isolated diamond crystals on the silicon surface at the edge of the deposited diamond film can be seen in Fig. 5(a). At this stage some of them are coalescing to form a continuous diamond film, which it is shown in Fig. 5(b).

Deposition on AISI 316 SS and AISI 304 SS after the described pretreatment, produced films in which diamond crystals were embedded in other carbon forms as can be seen from Fig. 6(a) for AISI 316 and (b) for AISI 304. The characteristic diamond peak at 1332 cm^{-1} is present together with two broad bands centered at 1350 and 1550 cm^{-1} indicating the presence of amorphous carbon with different degrees of graphitization. A slight insinuation of a band around 1140 and 1490 cm^{-1} are also noticeable. These bands have been the center of several discussions: though they were initially associated to nanocrystalline diamond carbon (NDC) [27] afterwards, many authors related them to trans-polyacetylene in diamond [28–30]. A SEM micrograph of a film obtained on AISI 316 SS is shown in Fig. 7.

In order to verify the influence of the pretreatment, deposits were performed under the same conditions on substrates on which the siliconization process was not concluded (i.e. after the first a-Si deposition and annealing process when no silicon signal was observed by Raman spectroscopy). The obtained films consist of mainly graphitized amorphous carbon, as can be seen from the

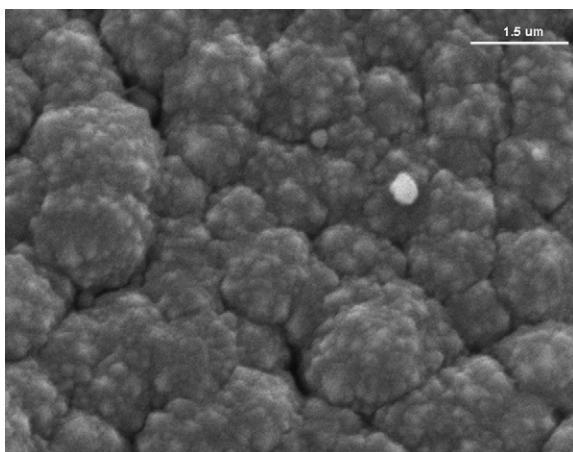


Fig. 7. SEM micrograph of a film deposited on AISI 316 SS. The thickness of the film is $3\text{ }\mu\text{m}$ and the deposition rate is $1\text{ }\mu\text{m/h}$.

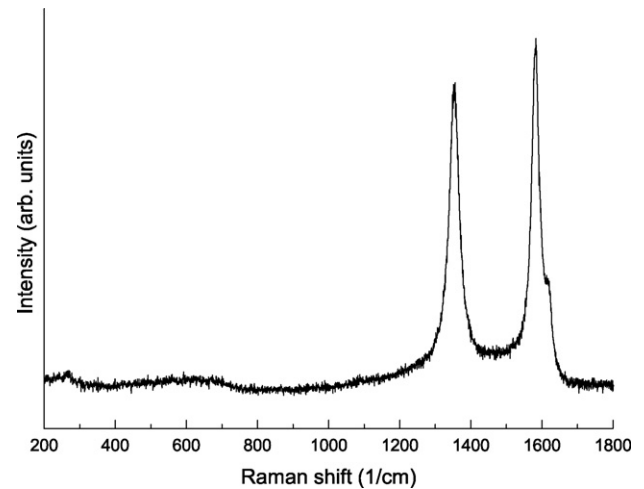


Fig. 8. Raman spectra of carbon film deposited on AISI 316 without a complete silicon diffusion process.

Raman spectrum in Fig. 8. The spectrum presents bands at 1350 and 1585 cm^{-1} , which are the D- and G-modes of disordered carbon. Together with the absence of the diamond peak (1332 cm^{-1}) this shows that silicon saturation is a prerequisite to deposit good quality diamond films. This is due to the fact that for low silicon concentrations, cementite forms on the surface of the steel samples and acts as a barrier for further carbon diffusion into the steel. This leads to graphite precipitation on the surface and, as cementite is unstable, iron from the cementite migrates through the graphite layer to the surface where it further enhances graphitization. When silicon reaches saturation concentration, SiC is formed which is stable in the presence of graphite, and thus inhibits graphitization of the surface [5,6,31].

4. Conclusions

From the results here presented it can be concluded that diamond growth on stainless steel is possible only after performing a pretreatment of the surface. A silicon diffusion process that leads to silicon saturation in the austenitic phase near the surface is indispensable. Thus, during diamond deposition, stable SiC forms on the surface and prevents iron from catalyzing graphitization at the surface of the stainless steel samples.

Polycrystalline diamond films were deposited on siliconized layers on AISI 304 and AISI 316 stainless steel substrates and on crystalline silicon wafers. Films deposited on silicon diffusion layers showed higher contents of non-diamond carbon phases such as amorphous carbon than films obtained on silicon. This fact has also been reported for diamond films grown on diffused boride layers in AISI 316 stainless steel by Buijnsters et al. [18].

Even small case depth silicon diffused layers, with depths in the range of barrier coatings thicknesses ($\sim 2\text{ }\mu\text{m}$), were sufficient to enable the possibility of successfully growing adherent diamond films on stainless steels.

Acknowledgements

We would like to thank to Alicia Petragalli for X-ray measurements and Marcelo Igarzábal for his technical assistance. This work was partially supported by SECyT grant PICT 38265.

References

- [1] P.W. May, Philos. Trans. R. Soc. Lond. A 15 (2000) 473.
- [2] X. Chen, J. Narayan, J. Appl. Phys. 74 (1993) 4168.

- [3] R. Haubner, A. Lindlbauer, B. Lux, *Diamond Relat. Mater.* 2 (1993) 1505.
- [4] R. Lux, R. Haubner, *Pure Appl. Chem.* 66 (1994) (1783).
- [5] H.-G. Jentsch, G. Rosenbauer, S.M. Rosiwal, R.F. Singer, *Adv. Eng. Mater.* 2 (2000) 369.
- [6] J.G. Buijnsters, P. Shankar, J.J. Ter Meulen, *Surf. Coat. Technol.* 201 (2007) 8955.
- [7] J.G. Buijnsters, P. Shankar, W.J.P. van Enkevort, J.J. Schermer, J.J. ter Meulen, *Phys. Stat. Sol. (a)* 195 (2003) 383.
- [8] C.R. Lin, C.T. Kuo, *Diamond Relat. Mater.* 7 (1998) 903.
- [9] I. Endler, A. Leonhardt, H.-J. Scheibe, R. Born, *Diamond Relat. Mater.* 5 (1996) 299.
- [10] J.G. Buijnsters, P. Shankar, W. Fleischer, W.J.P. van Enkevort, J.J. Schermer, J.J. ter Meulen, *Diamond Relat. Mater.* 11 (2002) 536.
- [11] L. Schäfer, M. Fryda, T. Stolley, L. Xiang, C.-P. Klages, *Surf. Coat. Technol.* 116–119 (1999) 447.
- [12] O. Gluzman, A. Hoffman, *Diamond Relat. Mater.* 6 (1997) 796.
- [13] J.C. Bareiß, G. Hackl, N. Popovska, S.M. Rosiwal, R.F. Singer, *Surf. Coat. Technol.* 201 (2006) 718.
- [14] H.-X. Zhang, Y.-B. Jiang, S. Yang, Z. Lin, K. Feng, *Thin Solid Films* 349 (1999) 162.
- [15] Y.S. Li, Y. Tang, Q. Yang, C. Xiao, A. Hirose, *Int. J. Refract. Met. Hard Mater.* 27 (2009) 417.
- [16] C. Bareiß, M. Perle, S.M. Rosiwal, R.F. Singer, *Diamond Relat. Mater.* 15 (2006) 754.
- [17] M. Gowri, H. Li, J.J. Schermer, W.J.P. van Enkevort, J.J. ter Meulen, *Diamond Relat. Mater.* 15 (2006) 498.
- [18] J.G. Buijnsters, P. Shankar, P. Gopalakrishnan, W.J.P. van Enkevort, J.J. Schermer, S.S. Ramakrishnan, J.J. ter Meulen, *Thin Solid Films* 426 (2003) 85.
- [19] H.L. Huang, T.Y. Lee, D. Gan, *Mater. Sci. Eng. A* 422 (2006) 259.
- [20] A. Nishimoto, K. Nakao, K. Ichii, K. Akamatsu, *Novel Materials Processing by Advanced Electromagnetic Energy Sources: Proceedings of the International Symposium on Novel Materials Processing by Advanced Electromagnetic Energy Sources, Osaka, Japan, (2005), p. 433.*
- [21] H.W. Grunling, R. Bauer, *Thin Solid Films* 95 (1982) 3.
- [22] H. Aikyo, K.-i. Kondo, *Jpn. J Appl. Phys.* 28 (1989) L1631.
- [23] A.A. Sirenko, J.R. Fox, I.A. Akimov, X.X. Xi, S. Ruvimov, Z. Liliental-Weber, *Solid State Commun.* 113 (2000) 553.
- [24] B.P. Swain, *Surf. Coat. Technol.* 201 (2006) 1132.
- [25] J.M. Perez, J. Villalobos, P. McNeill, J. Prasad, R. Cheek, J. Kelber, J.P. Estrera, P.D. Stevens, R. Glosser, *Appl. Phys. Lett.* 61 (1992) 563.
- [26] M.N. Islam, S. Kumar, *Appl. Phys. Lett.* 78 (2001) 715.
- [27] R.E. Shroder, R.J. Nemanich, J.T. Glass, *Phys. Rev. B* 41 (1990) 3738.
- [28] H. Kuzmany, R. Pfeiffer, N. Salk, B. Günther, *Carbon* 42 (2004) 911.
- [29] A.C. Ferrari, J. Robertson, *Phys. Rev. B* 63 (2001) 121405R.
- [30] A.J.S. Fernandes, M.A. Neto, F.A. Almeida, R.F. Silva, F.M. Costa, *Diamond Relat. Mater.* 16 (2007) 757.
- [31] Y.S. Li, A. Hirose, *Chem. Phys. Lett.* 433 (2006) 150.